© 2002 The Chemical Society of Japan

Synthesis, Solution Chemistry, X-ray Structure and Biological Activity of Novel Pyridoxal Thiosemicarbazone Derivatives

Marisa Belicchi Ferrari,* Franco Bisceglie, Enrico Leporati, Giorgio Pelosi, and Pieralberto Tarasconi

Dipartimento di Chimica Generale ed Inorganica, Chimica Analitica e Chimica Fisica,
Centro di Studio per la Strutturistica Diffrattometrica del CNR, Parco Area delle Scienze 17/A, 43100 Parma, Italy

(Received August 6, 2001)

Novel ligands were obtained by condensation of pyridoxal with thiosemicarbazides substituted with alkyl and aryl moieties on the aminic and/or hydrazinic nitrogen. The spectrophotometric characteristics of the various species are reported. The X-ray structure of two different dimethylthiosemicarbazones of pyridoxal — pyridoxal N^1,N^2-dimethylthiosemicarbazone monohydrate and pyridoxal N^1,N^1-dimethylthiosemicarbazone monohydrate — was determined. The change of methyl group position determines in the solid state strong differences which affect the ligand behavior of these compounds. In the first ligand, characterized by X-ray diffraction, the pyridoxal ring is in a zwitterion form, with the phenolic oxygen and the sulfur atoms in *trans* position to the iminic N atom. The second compound, with both methyl groups on the aminic nitrogen, shows the donor atoms SNO on the same side, making it potentially suitable for coordination to the metal. Biological studies have involved both inhibition of cell proliferation and apoptosis tests on human leukemia cell lines U937. Both ligands inhibited cell growth, but neither of them induced apoptosis. On the basis of the pK_a values, the second ligand is more easily dissociable and this allows us to predict the formation of neutral complexes with it.

In the course of our research in the area of anticancer compounds (non platinum therapeutic agents),[1,2] we have made attempts to compare the biological activities as well as the structure–activity relationships of new thiosemicarbazone compounds. We have synthesized and structurally characterized ligands, obtained by condensation of thiosemicarbazide with aromatic and aliphatic aldehydes, and several of their transition metal complexes.[3–10] We have also tested in vitro some biological properties on murine and human leukemic cell lines.[6,10]

As a continuation of this research program, new thiosemicarbazones containing substituents with different bulk and nature on the amino and hydrazino nitrogens have been synthesized to evaluate the influence of these substituents on the electronic properties, on the protonation equilibria and later on the biological activity. In particular in the present work we report the preparation and the UV–visible spectroscopic characterization of novel potential metal ligands obtained by condensation of the pyridoxal with thiosemicarbazides substituted with alkyl and aryl moieties. Also described are the X-ray structures of the ligands MeMe-HL·H_2O (pyridoxal N^1,N^2-dimethylthiosemicarbazone monohydrate) **1** and Me_2-H_2L·H_2O (pyridoxal N^1,N^1-dimethylthiosemicarbazone monohydrate) **2**. Trying to correlate structural data and biological activity, assays on inhibition of proliferation and on apoptosis were made for isomeric pyridoxal N^1 substituted ligands: N^1-ethylthiosemicarbazone Et-H_2L and N^1,N^1-dimethylthiosemicarbazone monohydrate Me_2-H_2L·H_2O **2**, on human erythroleukemic cell lines U937.

Experimental

General. Pyridoxal hydrochloride (99%), Aldrich, and thiosemicarbazides: 4-methylthiosemicarbazide and 4-phenyl-3-thiosemicarbazide (99%), Janssen; 4-ethyl-3-thiosemicarbazide (97%) and 4-allyl-3-thiosemicarbazide (97%), Aldrich; 2,4-dimethylthiosemicarbazide (98%), 4,4-dimethylthiosemicarbazide and 3-methylphenylthiosemicarbazide (99%), Lancaster, were commercially available. All materials and solvents were used without further purification.

Synthesis. The reaction between pyridoxal, in its neutral form, (0.1 g, 0.276 mmol) dissolved in proper solvent (40 mL), and substituted thiosemicarbazides (1 : 1 molar ratio), dissolved in the same solvent (30 mL), is reported in Scheme 1. The reactants were dissolved in the solvent and heated at the temperature and for the time reported in Scheme 2.

It was possible to isolate as crystals suitable for X-ray analysis only two of these compounds and namely MeMe-HL **1** and Me_2-H_2L **2**. In the reaction leading to the formation of Et-H_2L, if $EtOH_{abs}$ is used as the solvent, the anhydrous product is isolated, while if other solvents are used (water at different temperatures, EtOH/H_2O mixtures), the monohydrate product is separated. For the other thiosemicarbazones, the choice of different solvents does not modify the nature of the product but only its morphology.

Some analytical data for all compounds are reported below:

Me-H_2L·H_2O. Mp 180 °C. ^{1}H NMR (300 MHz, DMSO-d_6, TMS) δ 11.40 (bs, 1H, OH py), 9.93 (bs, 1H, NH-2), 8.59 (m, 2H, py CHN + NH-4), 7.93 (s, 1H, py), 5.29 (t, 1H, OH), 4.56 (d, 2H, py CH_2O), 2.99 (d, 3H, CH_3N), 2.42 (s, 3H, CH_3 py). MS (CI, CH_4) *m*/*z* (%) 255 (20) $[MH]^+$, 178 (18), 167 (23), 150 (100), 145 (11), 116 (8). Found: C, 43.3; H, 6.6; N, 20.8; S, 11.0%. Calcd for $C_{10}H_{16}N_4O_3S$: C, 44.1; H, 5.9; N, 20.6; S, 11.8%.

Et-H_2L. Mp 138 °C. ^{1}H NMR (300 MHz, DMSO-d_6, TMS) δ 11.63 (bs, 1H, OH py), 9.90 (m, 1H, NH-2), 8.57 (s, 1H, NH-4), 8.15 (s, 1H, py CHN), 7.99 (s, 1H, py), 5.28 (t, 1H, OH), 4.56 (d,

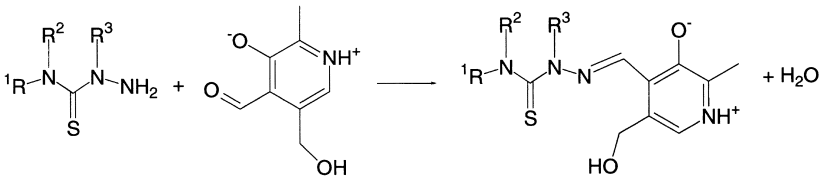

Scheme 1.

R^1	R^2	R^3	Compound	Solvent	Temp	Time (min)	Yield (%)
CH_3-	H-	H-	Me-$H_2L{\cdot}H_2O$	H_2O	40°C	120	65
CH_3CH_2-	H-	H-	Et-H_2L	$EtOH_{abs}$	reflux	50	72
CH_3-	H-	CH_3-	MeMe-HL·H_2O **1**	H_2O	r.t.	120	58
CH_3-	CH_3-	H-	Me_2-$H_2L{\cdot}H_2O$ **2**	MeOH	r.t.	50	69
CH_2=$CHCH_2$-	H-	H-	Allyl-$H_2L{\cdot}H_2O$	H_2O	reflux	45	71
	H-	H-	Ph-$H_2L{\cdot}H_2O$	EtOH 95%	r.t.	120	58
	H-	H-	Meph-$H_2L{\cdot}2H_2O$	H_2O	r.t.	20	82

Scheme 2.

2H, py CH_2O), 3.05 (m, 2H, CH_2), 2.40 (s, 3H, CH_3 py), 1.05 (t, 3H, CH_3). MS (CI, CH_4) *m/z* (%) 269 (23) $[MH]^+$, 251 (13), 178 (25), 166 (33), 150 (100). Found: C, 48.7; H, 6.3; N, 20.7; S, 11.8%. Calcd for $C_{11}H_{16}N_4O_2S$: C, 49.2; H, 6.0; N, 20.9; S 11.9%.

MeMe-HL·H_2O (1). Mp 201 °C. ^{1}H NMR (300 MHz, DMSO-d_6, TMS) δ 10.00 (bs, 1H, OH py), 9.20 (s, 1H, NH-4), 8.15 (s, 1H, py), 8.05 (s, 1H, CHN py), 5.45 (bs, 1H, OH), 4.63 (s, 2H, py CH_2O), 3.78 (s, 3H, CH_3 N-2), 3.00 (d, 3H, CH_3 N-1), 2.42 (s, 3H, CH_3Ar). MS (CI, CH_4) *m/z* (%) 269 (100) $[MH]^+$, 251 (47), 165 (23), 150 (40). Found: C, 45.5; H, 6.9; N, 20.2; S 11.5%. Calcd for $C_{11}H_{18}N_4O_3S$: C; 46.1; H, 6.3; N, 19.6; S, 11.2%.

Me_2-$H_2L{\cdot}H_2O$ (2). Mp 135 °C. ^{1}H NMR (300 MHz, DMSO-d_6, TMS) δ 11.68 (bs, 1H, OH py), 8.92 (s, 1H, NH-2), 8.60 (s, 1H, py), 7.94 (s, 1H, CHN py), 5.40 (bs, 1H, OH), 4.59 (s, 2H, py CH_2O), 2.42 (s, 3H, CH_3 py), 2.10 (s, 6H, $(CH_3)_2N$). MS (CI, CH_4) *m/z* (%) 268 (100) $[MH]^+$, 251 (50), 165 (34), 150 (63). Found: C, 45.7; H, 6.4; N, 19.2; S, 11.1%. Calcd for $C_{11}H_{18}N_4O_3S$: C, 46.1; H, 6.3; N, 19.6; S, 11.2%.

Allyl-$H_2L{\cdot}H_2O$. Mp 207.5 °C. ^{1}H NMR (300 MHz, DMSO-d_6, TMS) δ 11.67 (bs, 1H, OH py), 9.92 (bs, 1H, NH-2), 8.76 (bs, 1H, NH-4), 8.59 (s, 1H, py), 7.98 (s, 1H, CHN py), 5.89 (m, 1H, CH_2=C*H*–CH_2), 5.40 (m, 1H, OH), 5.12 (m, 2H, CH_2=CH–CH_2), 4.60 (d, 2H, py CH_2O), 4.21 (m, 2H, CH_2=CH–CH_2), 2.42 (s, 3H, CH_3 py). MS (CI, CH_4) *m/z* (%) 281 (83) $[MH]^+$, 263 (42), 178 (6), 167 (29), 150 (100), 115 (16). Found: C, 47.5; H, 6.2; N, 19.4; S, 11.1%. Calcd for $C_{12}H_{18}N_4O_3S$: C, 48.3; H, 6.1; N, 18.8; S, 10.7%.

Ph-$H_2L{\cdot}H_2O$. Dec. 136 °C. ^{1}H NMR (300 MHz, DMSO-d_6, TMS) δ 12.00 (bs, 1H, OH py), 10.37 (s, 1H, NH-2), 8.70 (s, 1H, NH-4), 8.00 (s, 1H, CHN py), 7.41 (m, 6H, Ar + py), 5.38 (bs, 1H, OH), 4.63 (s, 2H, py CH_2O), 2.44 (s, 3H, CH_3 py). MS (CI, CH_4) *m/z* (%) 297 (7) $[MH]^+$, 166 (42), 150 (46), 136 (100). Found: C, 53.0; H, 5.2; N, 17.2; S, 10.7%. Calcd for $C_{15}H_{18}N_4O_3S$: C, 53.9; H, 5.4; N, 16.7; S, 9.6%.

Meph-$H_2L{\cdot}2H_2O$. Mp 223 °C. ^{1}H NMR (300 MHz, DMSO-d_6, TMS) δ 11.99 (bs, 1H, OH py), 8.92 (s, 1H, NH-2), 8.70 (s, 1H, NH-4), 8.04 (s, 1H, CHN Ar), 7.39–7.30 (m, 4H, Ar), 7.10 (s, 1H, py), 5.39 (t, 1H, OH), 4.62 (d, 2H, py CH_2O), 2.45 (s, 3H, CH_3 py), 2.36 (s, 3H, CH_3 Ar). MS (CI, CH_4) *m/z* (%) 331 (4) $[MH]^+$, 164 (21), 150 (100). Found: C, 53.2; H, 5.8; N, 15.7; S, 8.3%. Calcd for $C_{16}H_{22}N_4O_4S$: C, 52.4; H, 6.0; N, 15.3; S, 8.7%.

Biological Data: Materials and Methods. U937 cells were seeded at 3×10^5/mL in the presence of RPMI supplemented with 5% of fetal bovine serum (FBS) and with antibiotics and treated with compounds Et-H_2L and Me_2-$H_2L{\cdot}H_2O$ (**2**). Both compounds were previously stored dry at room temperature and were dissolved in dimethyl sulfoxide (DMSO) just before their use. Cell mortality was evaluated on the fourth day by the trypan blue exclusion method and determined by using a hemocytometer. For the apoptosis assay U937 cells were seeded at 5×10^5/mL in the presence of the mentioned thiosemicarbazones at the concentrations used for the 40–50% cell proliferation inhibition. After 18 h the cells were washed with PBS at 2000 rpm for 10 min at 4 °C, and then 20 µL of a lysis buffer solution (EDTA 10 mM, Tris HCl 50 mM pH 8.0 and 0.5% (w/v) sodium laurylsarkosinate) were added. The pellet was subsequently redissolved and 2.5 µL of Proteinase K was added (4 mg/mL). After 1 h at 50 °C, 2.5 µg/mL of RNAse A (2 mg/mL) was added and incubated for 1 h at 40 °C

and then for 10 min at 70 °C. 10 µL of loading buffer (EDTA 10 mM pH 8.0, 1% agarose, 0.25% bromophenol blue, 40% sucrose) were subsequently added to the extracted DNA, which was loaded on the agarose gel (2%) with 0.1 µg/mL ethidium bromide to evaluate the characteristic effects of apoptosis by means of electrophoresis.

Instrumentation. Mass spectra measurements were carried out on a Finnigan 1020 model equipped with a quadrupole mass selector MATSSQ 710. Elemental C, H, N and S analyses were done on an automatic analyzer Carlo Erba model EA 1108 with gaschromatographic separation and revelation. The melting points were measured on a Gallenkamp instrument. IR spectra (KBr discs, 4000–400 cm^{-1}) were registered on a Fourier transformed Nicolet 5PC spectrophotometer. ^1H NMR results were obtained at room temperature on a Bruker AMX-300 spectrometer; chemical shifts are reported in ppm (δ) referenced to TMS (tetramethylsilane) as an internal standard. The compounds were dissolved in DMSO-d_6, giving rise to two signals at 2.5 and 3.4 ppm due to the dimethyl sulfoxide (DMSO) and water respectively. For UV-vis measurements, each solution (10^{-4}–10^{-5} mol dm^{-3}) to be measured was prepared by progressive addition of (1) a weighed amount of ligand, (2) an exact volume of hydrochloric acid to obtain the ligand in the protonated form and a sufficient amount of bidistilled water was added to make up the total volume V_o, which was 50.0 ± 0.01 cm^3. Measurements of pH were carried out with a fully automatic apparatus equipped with an Orion model 720A digital voltmeter and 5 cm^3 Metrohm E665 motor burette, both controlled by a Uvikon 941 PLUS spectrophotometer guided by a personal computer. The electrode combination consisted of a model OR (Orion Research) glass electrode (type 9101SC) and a model OR reference electrode (type 9002). In the cell the solution was thermostated, under purified nitrogen presaturated with water vapor at an ionic strength of 0.1 mol dm^{-3} (KCl), at 25 ± 0.1 °C and was passed through the spectrophotometric cuvette using a peristaltic pump. The electrode system was calibrated in terms of pH by using five fresh buffer solutions (pH 2.0, 4.0, 7.0, 9.0, 12.0). After each addition of KOH solution (0.2 mol dm^{-3}) at an ionic strength of 0.1 mol dm^{-3} (KCl), the pH was measured (range 2.4–12.5 pH) and the absorption spectra in the range 240–450 nm at 1 nm intervals were collected and recorded on a Uvikon 941 PLUS Kontron spectrophotometer using matched quartz cells of 1 cm pathlength against 0.1 mol dm^{-3} KCl as reference.

X-ray Crystallographic Studies. The crystal and instrumental parameters used in the unit cell-determination and in the data collection are summarized in Table 1. All intensity data were collected on an automated four-circle Philips diffractometer with Mo $K\alpha$ radiation for **1** and on a Siemens AED diffractometer with Cu $K\alpha$ radiation for **2** by the θ–2θ technique. No correction for absorption was applied for compound **1**, while in compound **2** a correction for absorption according to the method suggested by Sheldrick[11] was applied. The structures for both compounds were solved by SIR92.[12] In the final refinements all non-hydrogen atoms were anisotropically refined by least squares cycles using the SHELXL97[13] program for compound **1** and SHELXL93[14] for **2**. The hydrogen atoms, located on a difference map, were refined

Table 1. Experimental Data for the Crystallographic Analyses

Compounds	MeMe-HL·H_2O (**1**)	Me_2-H_2L·H_2O (**2**)
Formula	$C_{11}H_{18}N_4O_3S$	$C_{11}H_{18}N_4O_3S$
Molecular weight	286.348	286.348
Crystal system	monoclinic	monoclinic
Space group	$P2_1$	$P2_1/n$
a/Å	4.255(2)	9.898(3)
b/Å	13.226(3)	13.974(4)
c/Å	12.160(3)	10.459(3)
β/°	96.40(2)	107.10(4)
V/Å^3	680.0(4)	1383(1)
Z	2	4
D_{calc}/Mg m^{-3}	1.40	1.38
Radiation/Å	0.71069	1.54086
μ /cm^{-1}	2.5	21.9
F(000)	304.0	608.0
θ range/°	3 30	3 70
h range	−5 5	−11 11
k range	−18 18	0 16
l range	0 17	0 12
Standard reflection	−1 0 10	5 0 1
N° measured reflections	3035	2611
Maximum, minimum height in final ΔF map (eÅ^{-3})	0.22; −0.18	0.19; −0.21
N° refined parameters	244	242
N° unique reflections	1642	2085
R	0.027	0.049
w$R2$	0.065	0.142
Weights	$1/[\sigma^2(F_o)^2 + (0.0378P)^2 + 0.0P]$	$1/[\sigma^2(F_o)^2 + (0.0935P)^2 + 1.11P]$

$P = (\mathrm{Max}(F_o^2, 0) + 2F_c^2)/3$

Table 2. Selected Vibrational Bands (cm^{-1}) of Different Ligands

Ligand	ν(NH), ν(OH)	ν(NH)	ν(CH)	ν(C=N), ν(C=C)	Ring	δ(OH)	δ(NCS)	ν(C=S)
Me-$H_2L\cdot H_2O$	3383m,br	3135m	2954m	1532s	1507vs	1378s	1034s	921w
Et- H_2L	3409m 3269m	3168m	2965m	1606m	1503s	1376vs	1252s 1038s	923w
MeMe-$HL\cdot H_2O$ (**1**)	3329m,br 3248s,br	—	2935w	1547m	1508s 1431s	1378m	1055vs	920w
Me_2-$H_2L\cdot H_2O$ (**2**)	3404vs,br	3180mw,br	2922w	1560vs	1511m	1397s	1263s	—
Allyl-$H_2L\cdot H_2O$	3332ms,br	3133ms,br	2955m	1540vs	1508s	1383s	1210s 1030s	922m
Ph-$H_2L\cdot H_2O$	3299m,br	3129m,br	2955m	1597w 1540vs	1511s	1383s	1263m 1032ms	—
Meph-$H_2L\cdot 2H_2O$	3302m,br	3130m,br	2967m	1541vs	1511s	1383s	1030ms	917w

isotropically only for compound **1**. In ligand **2** all hydrogen atoms were located, except those of methyl groups; these were calculated with standard geometries. All calculations were performed on an ENCORE 91 computer of the Centro di Studio per la Strutturistica Diffrattometrica del CNR (Parma), geometrical calculations were carried out using PARST95,[15] ORTEP[16] and PLUTO[17] were used for the structure drawings. Atomic scattering factors were taken from Ref. 18.

Crystallographic data have been deposited at the CCDC, 12 Union Road, Cambridge CB2 1EZ, UK and copies can be obtained on request, free of charge, by quoting the publication citation and the deposition numbers CCDC 150213 and 150214, and the final atomic parameters, bond distances and angles have been deposited as Document No. 75008 at the Office of the Editor of Bull. Chem. Soc. Jpn.

Results and Discussion

Spectroscopy. IR spectra: Table 2 shows selected vibrational bands (cm^{-1}) of all the products. The ligands show a similar spectroscopic pattern comparable to that shown by the non-substituted H_2L.[3] For all compounds, the stretching vibrations of the NH (aminic) and OH (water, phenolic and hydroxymethyl) groups appear in the 3409–3248 cm^{-1} region, the absorption of the NH (hydrazinic) group occurring at lower wavenumbers. Differently from the other compounds, in the IR spectrum of Et-H_2L the absence of the bands due to the water of crystallization shows two sharp absorptions at 3409 and 3269 cm^{-1} assigned to the stretching mode ν(OH) and aminic ν(NH) respectively.

In compound **1**, the presence of intramolecular hydrogen bonds is displayed by the strong band at 3248 cm^{-1} attributed to the aminic group which is involved in interactions with an iminic nitrogen and an alcoholic oxygen. In **2** intramolecular hydrogen bonding –OH phenolic···N iminic causes the presence of the strong broad band at 3404 cm^{-1} and varies the intensity of the band ν(NH) at 3180 cm^{-1}, which appears weak as compared with the corresponding one of the other compounds. Only for allyl-H_2L an absorption at 2810 cm^{-1} (not reported in Table 2) can be clearly attributed to the NH^+ of the pyridine ring, whose protonation is a consequence of the migration of the hydrogen atom from the phenolic OH to the pyridine nitrogen,[3,19–21] while the same feature is not so clear for the other compounds. X-ray analysis of MeMe-$HL\cdot H_2O$ **1** reports the same protonation, but the molecular structure of Me_2-$H_2L\cdot H_2O$ **2** shows that this feature does not occur, as is however demonstrated by other pyridoxal derivatives.[22–25] No bands are observed at ca. 2500 cm^{-1} assignable to the SH group. The assignment of bands involving the C=S group is often uncertain and difficult owing to the large range (1300–700 cm^{-1}) in which the ν(C=S) band is generally found.[3,26] In our opinion this mode can be correctly attributed to the bands at ca. 920 cm^{-1}, but the generally weak intensity of the absorption of these bands does not allow attributions for all the ligands.

UV–vis spectra: all the cumulative protonation constants were obtained for the different ligands by refinement of several sets of absorption data with the computer programs SQUAD[27] and PHAB (included in the program package Hyperquad[28]). Typically the data contain the absorbance values, A_s, of a number of wavelengths for each of a number of equilibrium solutions of known analytical composition (pH and c_L). Assuming the standard definitions of K and β [$L + H^+ \rightleftarrows HL$, $\beta_1 = [HL]/[L][H^+]$ and $K^H{}_1 = \beta_1$, $L + 2H^+ \rightleftarrows H_2L$, $\beta_2 = [H_2L]/[L][H^+]^2$ and $K^H{}_2 = \beta_2/\beta_1$, $L + 3H^+ \rightleftarrows H_3L$, $\beta_3 = [H_3L]/[L][H^+]^3$ and $K^H{}_3 = \beta_3/\beta_2$, and so on] and that Beer's law is valid, for each solution and wavelength one can define the calculated absorbance A_s by Eq. 1, where ε_{pq} is the molar absorption coefficient for the species H_pL_q and l is the pathlength, the sum being extended over all the free and protonated species assumed to be present in solution:

$$A_{c,ik} = \ell \sum_0^p \sum_0^q \beta_{pq} [L]^p [H]^q \varepsilon_{pq} \quad (1)$$

In our case, p is always 1, so β_{pq} can be written as β_q and the equation becomes

$$A_{c,ik} = \ell \sum_0^q \beta_q [L][H]^q \varepsilon_q$$

The sum of square errors, used in the refinement procedure, is defined as in Eq. (2), m = number of solutions and n = number of wavelengths, $A_{o,ik}$ and $A_{c,ik}$ are the observed and calculated absorbances at the ikth point, with i referring to the solution and k to the wavelength.

$$U = \sum_{i=1}^{m} \sum_{k=1}^{n} |\Delta_{ik}|^2 = \sum_{ik} (A_{o,ik} - A_{c,ik})^2 \quad (2)$$

Table 3. Cumulative and Stepwise Protonation Constants of the Different Ligands at 25 °C and Ionic Strength 0.1 mol dm^{-3} (KCl), Obtained by the Computer Programs PHAB and SQUAD

	Me-H_2L	Et-H_2L	MeMe-HL	Me_2-H_2L	Allyl-H_2L	Ph-H_2L	Meph-H_2L
log β_1	11.67(1)	11.51(1)	8.54(1)	11.16(1)	11.58(1)	11.55(6)	10.84(1)
log β_1*	11.67(1)				11.58(1)		10.84(1)
log β_2	21.84(2)	21.38(2)	15.99(1)	19.36(1)	21.47(2)	22.07(7)	19.00(1)
log β_2*	21.86(3)				21.48(3)		18.97(1)
log β_3	30.18(2)	29.65(2)	20.47(1)	25.36(6)	29.74(2)	30.12(7)	25.16(2)
log β_3*	30.21(4)				29.75(4)		25.27(4)
log β_4	34.68(2)	34.00(2)	23.74(2)	30.39(6)	34.36(2)	34.49(7)	29.55(2)
log β_4*	34.71(4)				34.37(4)		29.64(4)
log K_1^H	11.67(1)	11.51(1)	8.54(1)	11.16(1)	11.58(1)	11.55(4)	10.84(1)
log K_2^H	10.17(2)	9.87(2)	7.45(1)	8.20(1)	9.89(2)	10.59(6)	8.16(1)
log K_3^H	8.34(2)	8.27(2)	4.28(1)	6.00(4)	8.27(2)	8.05(7)	6.16(2)
log K_4^H	4.50(2)	4.35(2)	3.27(2)	5.03(6)	4.62(2)	4.37(7)	4.39(2)
σ	$2.96\cdot10^{-3}$	$5.05\cdot10^{-3}$	$2.69\cdot10^{-3}$	$6.36\cdot10^{-3}$	$3.31\cdot10^{-3}$	$5.68\cdot10^{-3}$	$3.79\cdot10^{-3}$
σ*	$7.42\cdot10^{-3}$				$1.59\cdot10^{-2}$		$2.20\cdot10^{-2}$
U	$1.66\cdot10^{-2}$	$5.90\cdot10^{-2}$	$1.37\cdot10^{-2}$	$6.22\cdot10^{-2}$	$1.38\cdot10^{-2}$	$9.52\cdot10^{-2}$	$1.81\cdot10^{-2}$

*Overall protonation constants refined by PHAB program.

$\sigma^* = \left[\sum_{i=1}^{z} w_i (A_{o,i} - A_{c,i})^2 / (Z-m)\right]^{1/2}$, where m is the number of parameters to be refined, Z the total number of experimental absorbancy data and w_i is the weighting factor, used in the only in program PHAB.[28]

The mixed protonation constants obtained in this study are summarized in Table 3. All the protonation constants calculated by both computer methods (Table 3) agree closely, and the standard deviations of the refined quantities were very small. The different ligands have four protonation centers: the alcoholic oxygen (log K_1^H), the phenolic oxygen (log K_2^H), the hydrazinic nitrogen (log K_3^H) or sulfur group (tautomeric equilibrium in the thiol form) and the pyridine nitrogen (log K_4^H). All the overall and stepwise protonation constants for the various ligands are rather different from the corresponding ones of MeMe-HL, where, in agreement with the literature findings,[29] the probable presence of the sulfur atom in the protonated form increases the acidic character of all the other groups (alcoholic, hydrazinic and pyridinic). The inductive effect (+) of two adjacent methyl groups with the polarizability and resonance of the –C=S bond was used to explain this trend; moreover the log K_3^H, due to protonation of the sulfur atom (thiol form), is in good agreement with different mercapto derivatives with inductive effect (+), as well as the monosulfuric acid.

If the methyl group in compound Me-H_2L is replaced by an ethyl (Et-H_2L) or two methyl groups (Me_2-H_2L), the resulting functional groups are more acidic, as we can see by comparing the log β_n^H or log K_n^H values of the corresponding ligands. The presence of the methylphenyl group in Meph-H_2L or phenyl in Ph-H_2L instead of the methyl group seems to increase the acidic character of all functional groups (compare the log K_n^H values).

Typical absorption spectra (240–450 nm) for MeMe-HL (Fig. 1) and Me-H_2L (Fig. 2) are plotted in the range pH 3.007–6.715 and 6.250–9.092, respectively. When the pH increases from 3.007 to 6.715 (Fig. 1), combined hyperchromic-hypochromic and hypsochromic shifts are observed of the unique band in the range 334–346 nm [maximum, 0.867 A at 346 nm (1); maximum, 0.920 A at 344 nm (2); maximum, 0.933 A at 342 nm (3); maximum, 0.906 A at 340 nm (4); maximum, 0.870 A at 337 nm (5); maximum, 0.844 A at 336 nm (6); maximum, 0.810 A at 334 nm (7)]. In neutral and basic media the absorption spectra (Fig. 2) show mainly two bands: an intense peak (300–315 nm) shifting to shorter wavelength (hypsochromic effect) with decreasing intensity (hypochromic effect) and a weaker band in the range 377–385 nm [maxima, 1.036 A at 315 nm (1) and 0.944 A at 385 nm (1); maxima, 1.001 A at 300 nm (5) and 0.936 A at 377 nm (5)].

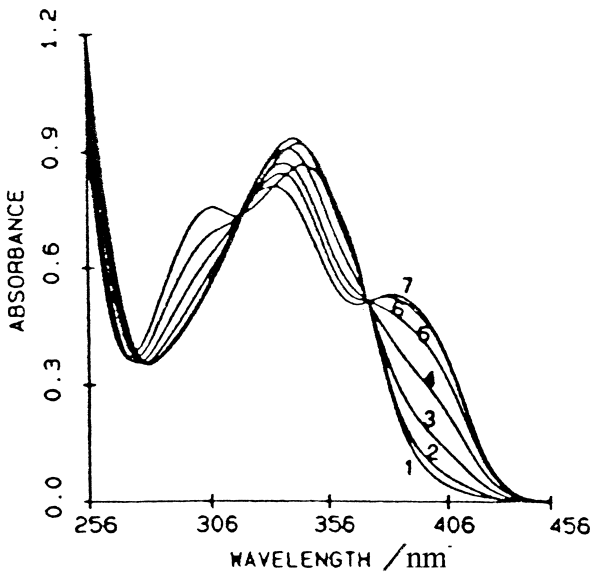

Fig. 1. Plots of experimental absorbance data versus wavelength for solutions [C_L 9.3×10^{-4}–6.9×10^{-4} mol dm^{-3}; pH 3.007 (**1**), 3.543 (**2**), 4.066 (**3**), 4.573 (**4**), 5.077 (**5**), 5.719 (**6**), 6.715 (**7**)] for MeMe-HL at 25 °C and ionic strength 0.1 mol dm^{-3} (KCl).

When the absorption spectra at various pH values (at constant ligand concentration) are compared, sharp isosbestic

Table 4. Molar Extinction Coefficient Maxima (ε_{max}) of the Absorbing Species at Equilibrium and Isosbestic Points for the Different Ligands

	Me-H_2L	Et-H_2L	MeMe-HL	Me_2-H_2L	Allyl-H_2L	Ph-H_2L	Meph-H_2L
	λ/nm ($\varepsilon\cdot10^{-3}$)	λ/nm ($\varepsilon\cdot10^{-3}$)	λ/nm ($\varepsilon\cdot10^{-3}$)	λ/nm ($\varepsilon\cdot10^{-3}$)	λ/nm ($\varepsilon\cdot10^{-3}$)	λ/nm ($\varepsilon\cdot10^{-3}$)	λ/nm ($\varepsilon\cdot10^{-3}$)
ε_L	381; (19.14)	380; (17.34)	313; (8.600) 366; (5.373)	383; (18.56)	381; (18.63)	388; (17.73)	388; (18.95)
ε_{HL}	297; (12.60) 375; (12.05)	297; (12.85) 376; (11.31)	321; (8.941) 383; (5.675)	370; (12.94)	244; (13.83) 299; (12.19) 376; (11.92)	303; (10.29) 386; (16.35)	303; (11.39) 378; (11.98)
ε_{H_2L}	298; (13.19) 376; (12.54)	298; (13.05) 378; (12.15)	245; (15.76) 336; (9.113) 383; (5.827)	298; (14.38)	298; (12.42) 377; (12.25)	303; (12.06) 377; (13.12)	315; (12.41) 389; (10.55)
ε_{H_3L}	257; (12.21) 316; (13.33) 386; (12.20)	314; (12.71) 386; (12.12)	343; (10.93)	299; (14.07)	257; (11.37) 316; (12.06) 386; (12.28)	255; (13.10) 315; (12.87) 389; (11.66)	256; (14.05) 315; (12.85) 390; (11.16)
ε_{H_4L}	351; (19.71)	351; (16.89)	304; (8.944) 349; (8.524)	317; (17.45)	353; (16.79)	354; (16.73)	354; (16.81)
Isosbestic Points λ / nm	258; 270; 307; 356; 385	252; 267; 349; 371	319; 372	249; 302; 373	307; 376; 424	279; 285; 301	252; 276; 302 392;

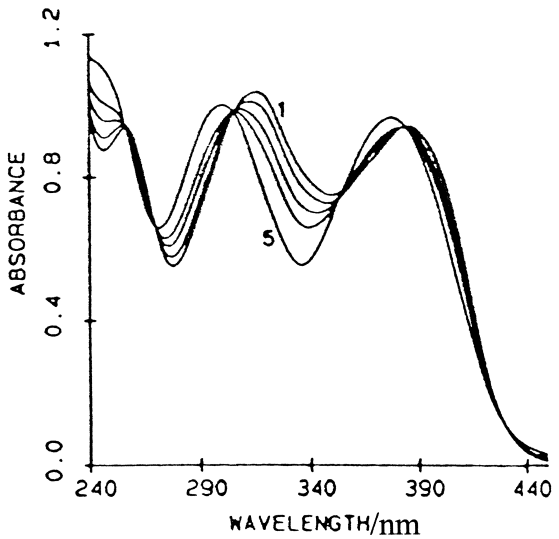

Fig. 2. Plots of experimental absorbance data versus wavelength for solutions [C_L 9.1×10^{-4}–7.2×10^{-4} mol dm^{-3}; pH 6.250 (**1**), 7.489 (**2**), 8.005 (**3**), 8.329 (**4**), 9.092 (**5**)] for Me-H_2L at 25 °C and ionic strength 0.1 mol dm^{-3} (KCl).

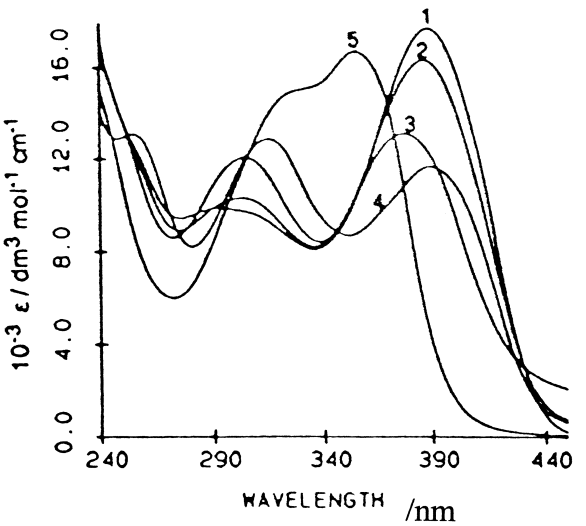

Fig. 3. Plots of the molar absorption coefficients (ε) of the five species of Ph-H_2L: (**1**) ε_L, (**2**) ε_{HL}, (**3**) ε_{H_2L}, (**4**) ε_{H_3L}, (**5**) ε_{H_4L}.

points in the Fig. 1 (319 nm, 372 nm) and Fig. 2 (258 nm, 270 nm, 307 nm, 356 nm, 385 nm) are observed. The presence of these points of constant absorption suggests that the simultaneous equilibria are altered by pH, and moreover indicates the coexistence of several species at equilibrium in solution.

In Fig. 3 the molar absorption coefficients of the five species for Ph-H_2L obtained by using the program SQUAD are plotted in the range 240–450 nm. By means of the positions of the absorption maxima (Table 4) it is possible to check the contribution of each species to the whole spectrum.

Crystal Structures. In compound MeMe-HL·H_2O (pyridoxal N^1,N^2-dimethylthiosemicarbazone monohydrate) **1**, the pyridoxal ring is present as a zwitterion, where the nitrogen atom is protonated and the phenolic oxygen is deprotonated. The aminic nitrogen atom N1 is intramolecularly linked to both N3 and O2 (alcoholic) atoms, stabilizing in this way the molecular conformation characterized by a strong distortion (the dihedral angle between the pyridine ring and the thiourea group is 33.08(4)°). The phenolic oxygen and the sulfur atom are both in *trans* position to N3 (Fig. 4).

A comparison of the bond distances in the side chain (Table 5) with those previously reported for unsubstituted pyridoxal thiosemicarbazone[3] and its copper complexes[7,10] reveals a small delocalization of the system. Bond distances and angles in the pyridoxal ring agree well with those present when the same moiety adopts the zwitterion form. The C5–N4–C6 angle of the pyridine ring [124.1(1)°] is characteristic of a protonated nitrogen.[3] This feature is also in agreement with the O1–C7 distance [1.287(2) Å], intermediate between a single (1.43 Å) and double bond (1.23 Å), and with the N4···O1W($-x$, 1/2 + y, 1$-z$) distance [2.697(2) Å, 170(2)°] corresponding to an intermolecular hydrogen bond. The packing is characterized

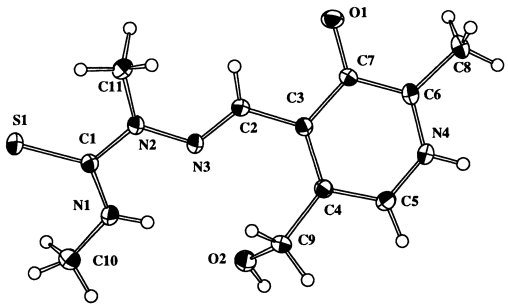

Fig. 4. ORTEP drawing of ligand **1** showing the atomic numbering scheme.

Table 5. Comparison of Bond Distances (Å) for New Ligands and Unsubstituted H_2L

	H_2L[3]	MeMe-HL·H_2O (**1**)	Me_2-H_2L·H_2O (**2**)
S1–C1	1.70(1)	1.675(2)	1.686(2)
O1–C7	1.29(1)	1.287(2)	1.350(3)
O2–C9	1.43(1)	1.423(2)	1.410(3)
N1–C1	1.33(1)	1.323(2)	1.336(3)
N1–C10		1.446(3)	1.464(4)
N1–C11			1.463(3)
N2–N3	1.40(1)	1.368(2)	1.362(3)
N2–C1	1.35(1)	1.385(2)	1.372(3)
N2–C11		1.450(2)	
N3–C2	1.30(1)	1.274(2)	1.275(2)
N4–C5	1.36(1)	1.348(2)	1.341(3)
N4–C6	1.34(1)	1.334(2)	1.334(4)
C2–C3	1.45(1)	1.467(2)	1.463(3)
C3–C4	1.42(1)	1.405(2)	1.414(4)
C3–C7	1.44(1)	1.431(2)	1.413(3)
C4–C5	1.37(1)	1.375(2)	1.382(3)
C4–C9	1.52(1)	1.517(3)	1.508(4)
C6–C7	1.42(1)	1.417(2)	1.399(3)
C6–C8	1.50(1)	1.487(3)	1.505(4)

by ligand molecules joined by O2···S($-x$, 1/2 + y, $2-z$) hydrogen bonds [3.296(2) Å, 172(4)°] to form chains running along the screw axis parallel to b. These chains are connected through the above mentioned N4···O1W bond. Moreover the water molecules are involved in two hydrogen bonds: the first with the phenolic oxygen O1 of the ligand in general position (2.683(2) Å) and the second (2.742(2) Å) with the same atom O1 of the molecule shifted of a unit along a. So sheets of thiosemicarbazonic moieties are alternated with sheets of aromatic rings and water molecules.

The compound Me_2-H_2L·H_2O **2** (pyridoxal N^1,$N^{1\prime}$-dimethylthiosemicarbazone monohydrate) with both methyl groups on the aminic nitrogen shows the donor atoms SNO on the same side, in a suitable position for the coordination to the metal. This conformation is probably determined by an intramolecular hydrogen bond between the protonated phenolic oxygen and the hydrazinic N3 atom (Fig. 5). Differently from ligand **1** the C5–N4–C6 angle (118.6(3)°) of the pyridine ring is smaller than 120° according to a not protonated form. The whole system is more planar (the dihedral angle between the pyridine ring and the thiourea moiety is 6.78(7)°). The packing is determined by an extensive network of hydrogen bonds involving the crystallization water molecule, the alcoholic O2 atom, the protonated hydrazinic N2. In both compounds **1** and **2** the N–H···S hydrogen bonds, present in several thiosemicarbazones and in the unsubstituted pyridoxal thiosemicarbazone, are absent.

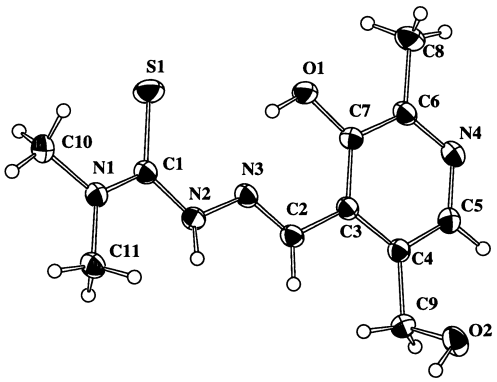

Fig. 5. ORTEP drawing of compound **2** showing the atomic numbering scheme.

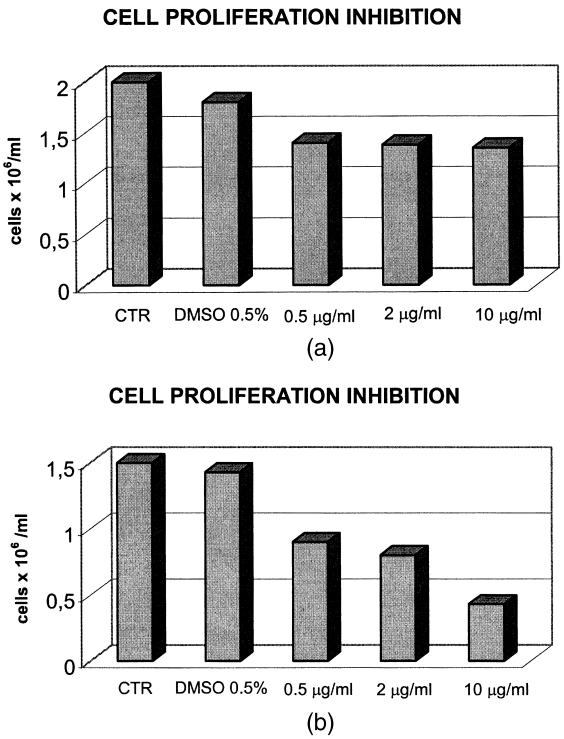

Fig. 6. Effects of Et-H_2L (a) and Me_2-H_2L·H_2O (b) on U937 proliferation on the 4th day.

Biological Tests: Effects on Cell Proliferation and Apoptosis Induction. In Fig. 6 are reported effects of Et-H_2L (a) and Me_2-H_2L·H_2O **2** (b) on U937 proliferation on the fourth day at different values of concentration. Ligands Et-H_2L and Me_2-H_2L·H_2O (**2**) have been tested in vitro. U937 human leukemic cell lines have been used, and we focused the biological activity relatively at *cell proliferation inhibition* and *apoptosis induction*, because a number of anticancer drugs may exert their activity by inducing *apoptosis*.[30] Up to now we selected only two ligands because we wanted to evaluate the biological effect of the different alkylic chain on nitrogen N1 for two isomeric compounds. Both ligands utilized at 10 μg/mL inhibited

cell proliferation of 33% (Et-H_2L) and 70% (Me_2-$H_2L \cdot H_2O$) as can be observed from the cell growth diagrams reported in Fig. 6. When the action of the compounds increases, the cell growth decreases and the corresponding histogram shows a lower bar. Using these compounds at the minimum concentration values at which the maximum inhibition was observed, we see that no one of them was able to cause the typical DNA fragmentation; therefore, they did not induce apoptosis.

The authors acknowledge the Italian MURST (COFIN 2001) that financially supported the work in the frame of the project "Inorganic Compounds as Selective Antitumoral Drugs: Molecular Targets and Biological Models" (coordinator Prof. I. Viano). The authors are also grateful to Dr. R. Albertini and S. Pinelli of the Institute of Medical Special Pathology, University of Parma, for the biological assays.

References

1 S. B. Padhyé and G. B. Kaufmann, *Coord. Chem. Rev.*, **63**, 127 (1985).

2 D. X. West, A. E. Liberta, S. B. Padhyé, R. C. Chikate, P. B. Sonawane, A. S. Kumbhar, and R. G. Yerande, *Coord. Chem. Rev.*, **123**, 49 (1993).

3 M. Belicchi Ferrari, G. Gasparri Fava, E. Leporati, C. Pelizzi, P. Tarasconi, and G. Tosi, *J. Chem. Soc., Dalton Trans.*, **1986**, 2455.

4 M. Belicchi Ferrari, G. Gasparri Fava, P. Tarasconi, and C. Pelizzi, *J. Chem. Soc., Dalton Trans.*, **1989**, 361.

5 M. C. Rodríguez-Argüelles, M. Belicchi Ferrari, G. Gasparri Fava, C. Pelizzi, G. Pelosi, R. Albertini, A. Bonati, P. P. Dall'Aglio, P. Lunghi, and S. Pinelli, *J. Inorg. Biochem.*, **66**, 7 (1997).

6 M. Belicchi Ferrari, G. Gasparri Fava, E. Leporati, G. Pelosi, R. Rossi, P. Tarasconi, R. Albertini, A. Bonati, P. Lunghi, and S. Pinelli, *J. Inorg Biochem.*, **70**, 145 (1998).

7 M. Belicchi Ferrari, G. Gasparri Fava, C. Pelizzi, P. Tarasconi, and G. Tosi, *J. Chem. Soc., Dalton Trans.*, **1987**, 227.

8 M. Belicchi Ferrari, G. Gasparri Fava, M. Lanfranchi, C. Pelizzi, and P. Tarasconi, *Inorg. Chim. Acta*, **181**, 253 (1991).

9 M. Belicchi Ferrari, G. Gasparri Fava, C. Pelizzi, and P. Tarasconi, *J. Chem. Soc., Dalton Trans.*, **1992**, 2153.

10 M. Belicchi Ferrari, G. Gasparri Fava, P. Tarasconi, R. Albertini, S. Pinelli, and R. Starchich, *J. Inorg. Biochem.*, **53**, 13 (1994).

11 S. Parkin, B. Moezzi, and H. Hope, *J. Appl. Crystallogr.*, **28**, 53 (1995).

12 A. Altomare, G. Cascarano, C. Giacovazzo, A. Guagliardi, M. C. Burla, G. Polidori, and M. Camalli, SIR 92, a program for automatic solution of crystal structures by direct methods. *J. Appl. Crystallogr.*, **27**, 435 (1994).

13 G. M. Sheldrick, SHELXL 97, University of Gottingen, Germany (1996).

14 G. M. Sheldrick, SHELXL 93, A Program for Structure Refinement, University of Gottingen, Germany (1993).

15 M. Nardelli, *Comput. Chem.*, **7**, 95 (1983).

16 C. K. Johnson, ORTEP Fortran Thermal-Ellipsoid Program for Crystal Structure Illustrations, Report ORNL-3794, Oak Ridge National Laboratory (1965).

17 W. D. S. Motherwell, PLUTO, University of Cambridge (1976).

18 International Tables for X-ray Crystallography, Kynoch Press, Birmingham (1975), vol. 4.

19 P. Domiano, A. Musatti, M. Nardelli, C. Pelizzi, and G. Predieri, *Transition Met. Chem.* (London), **4**, 351 (1979).

20 Y. Matsushima, *Chem. Pharm. Bull.*, **16**, 2143 (1968).

21 S. P. Mital, R. V. Singh, and J. P. Tandon, *J. Inorg. Nucl. Chem.*, **43**, 3187 (1981).

22 J. P. Souron, M. Quarton, F. Robert, A. Lyubchova, A. Cosse-Barbi, and J. P. Doucet, *Acta Crystallogr., Sect. C*, **51**, 2179 (1995).

23 K. S. McCully, and G. B. Carpenter, *Acta Crystallogr., Sect. C*, **43**, 2345 (1987).

24 R. K. Sharma, R. V. Singh, and J. P. Tandon, *J. Inorg. Nucl. Chem.*, **42**, 463 (1980).

25 M. F. Iskander and L. El-Sayed, *J. Inorg. Nucl. Chem.*, **33**, 4253 (1971).

26 D. M. Wiles and T. Suprunchuk, *Can. J. Chem.*, **46**, 1865 (1968).

27 D. J. Leggett and W. A. E. McBryde, *Anal Chem.*, **47**, 1065 (1975).

28 A. Sabatini, A. Vacca, and P. Gans, *Coord. Chem. Rev.*, **120**, 389 (1992).

29 F. G. Bordwell and G. Z. Ji, *J. Am. Chem. Soc.*, **113**, 8398 (1991).

30 A. G. Eliopoulos, D. J. Kerr, J. Herod, L. Hodgkins, S. Krajewsk, J. C. Reed, and L. S. Young, *Oncogene*, **7**, 1217 (1995).